



HAL
open science

Deterministic Integration of Quantum Emitters by Direct Laser Writing using Two-Photon Polymerization

Xiaolun Xu, Aurélie Broussier, Mackrine Nahra, Fabien Geoffray, Ali Issa, Safi Jradi, Renaud Bachelot, Christophe Couteau, Sylvain Blaize

► **To cite this version:**

Xiaolun Xu, Aurélie Broussier, Mackrine Nahra, Fabien Geoffray, Ali Issa, et al.. Deterministic Integration of Quantum Emitters by Direct Laser Writing using Two-Photon Polymerization. 2020. hal-02434901

HAL Id: hal-02434901

<https://hal.science/hal-02434901>

Preprint submitted on 10 Jan 2020

HAL is a multi-disciplinary open access archive for the deposit and dissemination of scientific research documents, whether they are published or not. The documents may come from teaching and research institutions in France or abroad, or from public or private research centers.

L'archive ouverte pluridisciplinaire **HAL**, est destinée au dépôt et à la diffusion de documents scientifiques de niveau recherche, publiés ou non, émanant des établissements d'enseignement et de recherche français ou étrangers, des laboratoires publics ou privés.

Deterministic Integration of Quantum Emitters by Direct Laser

Writing using Two-Photon Polymerization

Xiaolun Xu[†], Aurélie Broussier[†], Mackrine Nahra[†], Fabien Geoffray[‡], Ali Issa[†], Safi Jradi[†],
Renaud Bachelot[†], Christophe Couteau^{*†}, Sylvain Blaize^{*†}

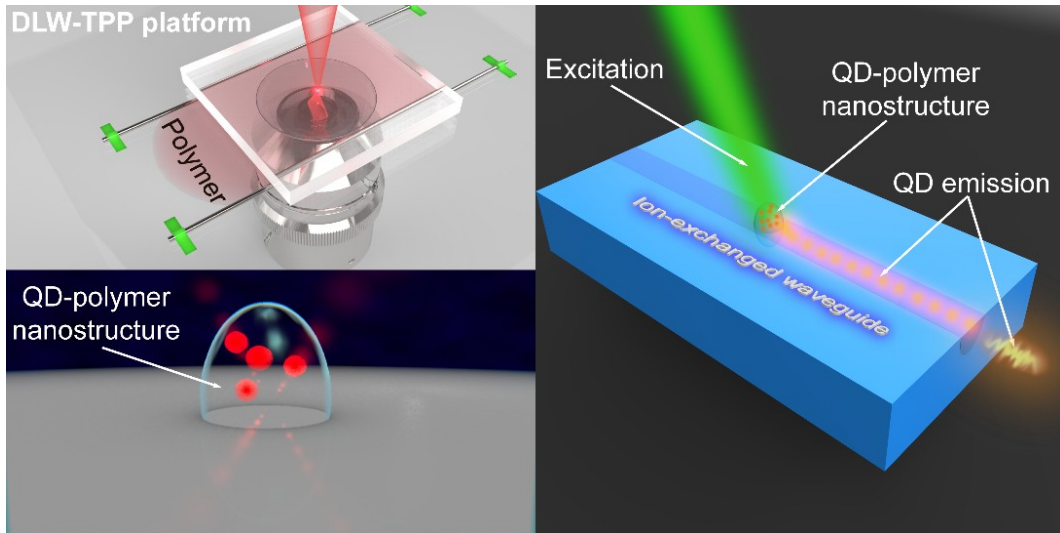
[†]*Light, nanomaterials, nanotechnologies (L2n), ERL 7004, CNRS. University of Technology of Troyes, 12 rue Marie Curie, 10004 Troyes Cedex, France*

[‡]*Teem Photonics, 61 Chemin du Vieux Chêne, 38246 Meylan, France*

ABSTRACT: A major challenge towards integrated quantum optics is the deterministic integration of quantum emitters on optical chips. Combining the quantum optical properties of some emitters with the benefits of integration and scalability of integrated optics is still a major issue to overcome. In this work, we demonstrate a novel approach in which quantum emitters are positioned in a controlled manner onto a substrate and onto an optical waveguide with nanoscale precision via direct laser writing based on two-photon polymerization (DLW-TPP). Our quantum emitters are colloidal CdSe/ZnS quantum dots (QDs) embedded in polymeric nanostructures. Varying the laser parameters during the patterning process, size-controlled QD-polymer nanostructures have been characterized systematically. Structures as small as 20 nm in height were fabricated. The well-controlled QD-polymer nanostructure systems were then successfully integrated at will onto a photonic platform, in our case, ion exchange waveguide (IEW). We show that our quantum dots maintain their high light emitting quality after integration as verified by photoluminescence (PL) measurements. Ultimately, QD emission coupled to our waveguides is detected through a home-build fiber-edge coupling PL measurement setup. Our results show the potential for future quantum optical communications and pave a novel way towards top-down deterministically integrating quantum emitters onto complex photonic chips.

KEYWORDS: integrated quantum optics, quantum emitters, quantum dots, photopolymers, two photon polymerization, waveguide

■ [TOC Graphic](#)



Luminescent colloidal semiconductor quantum dots (QDs) have already proven to be promising solid-state quantum emitters in the fields of nanophotonics and quantum optics.¹⁻⁸ For the practical realization of such scalable photonic quantum devices, one of the key requirements is the ability to integrate quantum dots onto specific optical chip locations. Many approaches have been explored, including electron beam lithography (EBL),⁹⁻¹² capillary force,^{13,14} optical trapping,^{15,16} and atomic force microscopy transfer methods.^{17,18} However, these methods have some limitations such as complicated operations, high manufacturing costs and multiple fabricating steps.^{19,20}

Direct laser writing based on two-photon polymerization DLW-TPP has been employed for producing 1D, 2D and 3D arbitrary microscale and even nanoscale polymeric structures in a fast and simple manner with high positioning and laser writing accuracy.²¹⁻²⁴ In conventional DLW-TPP process, a pulsed laser is tightly focused to a diffraction-limited spot within the volume of liquid photopolymers. Due to a two-photon absorption (TPA) process,²⁵ photo-polymerization (crosslinking of photopolymer) is triggered to form arbitrary hollow 3D polymeric structures by scanning the laser. Recently, embedding quantum dots into a photopolymer host matrix has been exploited to produce QD-polymer nanocomposites by photopolymerization, which joins the active light-emitting property of QDs together with the technological feasibilities of the polymer matrix.²⁶⁻²⁹ However, optical devices integrated with QD-polymer nanocomposites via DLW-TPP have not been reported.

In this work, for the first time, we demonstrate the deterministic integration of photonic devices with quantum emitters via DLW-TPP. A development of conventional DLW-TPP platform enables transferring of size-controlled QD-polymer nanocomposites onto preselected optical substrates with nanometer-scale precision. We succeeded in creating single QD-polymer nanostructures at the center of ion exchanged waveguides. The quantum dot emission coupled to an ion exchanged waveguide (IEW) is demonstrated via photoluminescence measurement. This work indicates good prospects toward practical realizations of deterministic integration of quantum emitters onto complex photonic devices.

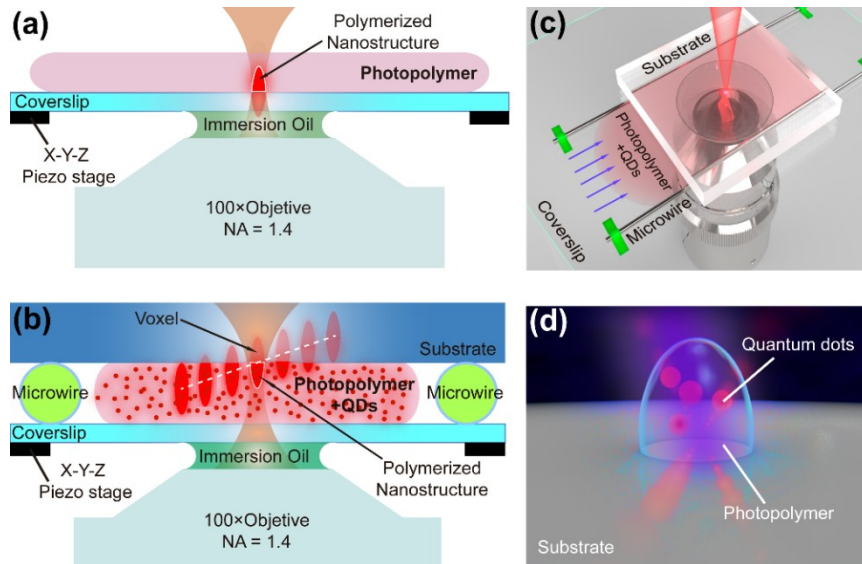


Figure 1. Schematic of conventional DLW-TPP platform. (b, c) Cross-section and 3D Illustration of developed DLW-TPP platform. Red dots represent quantum dots dispersed inside photopolymer. White dashed line shows controlling of laser focus height. (d) Conceptual a single QDs-polymer voxel integrated on a substrate.

Standard DLW-TPP process is executed with a Nanoscribe Professional GT printer,^{30,31} which is powered by a femtosecond near-infrared laser at 780 nm, operating with ~ 100 fs pulse duration and 80 MHz repetition rate and a maximum mean power of $P_{max} \approx 20$ mW (measured after the focusing objective). Photoresist is drop-casted on a $22 \times 22 \times 0.17$ mm³ transparent glass coverslip mounted on x-y-z piezoelectric translation stages imaged by a 100 \times immersion oil high resolution optical microscope objective, as shown in Figure 1.(a). In this conventional DLW-TPP configuration, a typical working distance of the oil immersion objective is less than 170 μ m, which makes this approach to be used only for thin substrates. If one wants to use on another substrate containing waveguides in plane or a silicon on insulator (SOI) substrate, some developments are necessary in order to do DLW-TPP. Bückmann *et al.* proposed dipping the microscope objective directly into a special photoresist material.³² However, commercially available oil immersion-type microscope objectives are not designed for direct use with the photoresist material instead of the immersion oil. Moreover, diversity of substrate shapes and sizes limits its mounting to standard substrate holders. Thus, a need exists for developing a DLW-TPP configuration that can transfer QD-polymer nanocomposites onto thicker optical substrates.

Here, we developed a DLW-TPP platform configuration for integrating QD-polymer nanocomposites on complex photonic chips, as shown in Figure 1.(b, c). First of all, two tungsten microwires with 25 μ m diameters are placed directly between a coverslip and a face-down thick glass substrate for creating a free space. Secondly, a homemade photopolymer (pentaerythritol triacrylate monomer) resist containing colloidal CdSe/ZnS quantum dots is placed into the space thanks to the capillary force. Then the laser is focused at the interface between polymer and substrate during the patterning process. Finally, the non-exposed parts of photopolymer liquids are subsequently removed in an acetone solution, resulting in a QD-polymer nanocomposite on the thick substrate. A QD-polymer nanocomposite fabricated by standard or developed DLW-TPP is depicted schematically in Figure 1.(d).

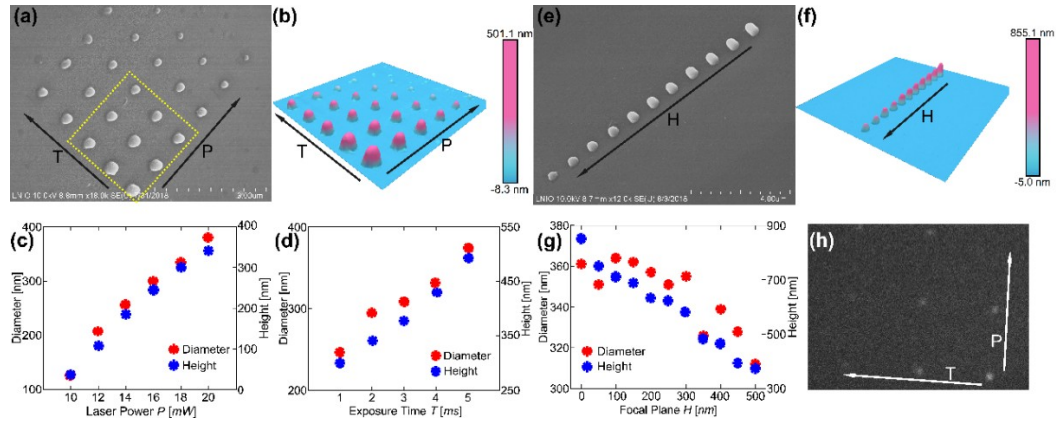


Figure 2. Characterization of QD-polymer voxels. (a) Tilt-view SEM image of a voxel array by changing laser power P (10 – 20 mW with a step of 2 mW) and exposure time T (1 – 5 ms with a step of 1 ms). The default value H in this sample is 0 nm. (b) 3D AFM image of the array of single voxel structures of the same sample with (a). (c, d) Dependency of the height and diameter of single voxel structures in function of P , T respectively. $T = 5$ ms in (c), $P = 20$ mW in (d). (e) Tilt-view SEM image of an array of voxel structures by only changing the focal plane H (0 - 500 nm with a step of 50 nm). (f) 3D AFM image of the array of single voxel structures of the same sample with (e). (g) Size controlling by adjusting H with $P = 20$ mW and $T = 5$ ms . (h) Measured PL image of a voxel array, marked with the dashed yellow square in (a).

Parametric study on fabricating QD-polymer nanocomposites by this developed DLW-TPP was then performed. The ellipsoidal-shape volume of photo-polymerized resist inside the focused laser beam, called voxel, represents the ultimate resolution reachable during the DLW fabrication. Previous efforts for improving the precision of voxels by changing laser writing power P and laser exposure time T have been demonstrated on conventional DLW-TPP platform.^{33–35} Herein, to show the high fabricating accuracy of our developed platform with QD-polymer nanostructures, we systematically investigate the dependence of the size of the QD-polymer nanostructures by a fabricated array of 6×5 voxels (with pitches of 1 μm) on silica substrates while adjusting P and T . Our process also shows great repeatability and high yield. Figure 2.(a, b) show, respectively, scanning electron microscopy (SEM) and atomic force microscopy (AFM) images of the QD-polymer nanostructure voxels fabricated on the substrate. Clearly, by adjusting laser power and exposure time, the diameter and height of the voxels can be controlled with high spatial accuracy. The dependence of P on the voxel dimensions (diameter and height) is shown in Figure 2.(c). The dimension of voxel structures can be scaled down to ~ 20 nm in height and ~ 126 nm in diameter (with $P=10$ mW , $T=1$ ms), in this case, only few quantum dots are trapped inside the polymeric voxel considering that the average quantum dot diameter is typically around 10 nm. Moreover, the relationship between voxel size with exposure time is shown in Figure 2.(d). As expected, diameter and height decrease along with the decreasing of T . Consequently, this is an efficient way of controlling the volume of voxels by carefully adjusting P and T to control the amount of energy applied to the QD-polymer resin. In addition, as shown in Figure 1.(b), the DLW-TPP equipped with x-y-z movement stage allows tuning the laser focal position H during the patterning process. We thus fabricated an array of QD-polymer voxels to investigate the possibility for further reducing the voxel size, as shown in Figure 2.(e, f). The dependences of the voxel size on H is shown in Figure 2.(g). In this case, we also demonstrate our ability to fabricate QD-polymer

structures with different shapes, such as lines, squares and cube (shown in Supporting Information Section S1).

Due to the importance in defining the fluorescence properties of the quantum dots, we measured the photoluminescence (PL) emitted by each voxel. For that, we made an array of QD-polymer voxels with longer distances between the voxels (5 μm) in order to avoid illumination from the neighboring voxels. Figure 2.(h) shows far-field fluorescence image of the array excited by an LED source emitting at 450 nm within a $\approx 30 \times 10 \mu\text{m}^2$ field of view. The emitting light was filtered by a 530 nm long-pass filter and recorded by an Electron-Multiplying CCD camera. Bright points with different intensities are clearly visible and correspond to the quantum dot emission from voxels with different volumes. As we can control the size of the voxels at will, we can therefore control the number of quantum dots inside a given voxel. We point out the potential of this control for the practical integration of single QDs into these polymer nanostructures that can be positioned onto specific photonic devices by simply changing the voxel volume, specifically by adjusting P , T and H . Another approach for reducing QD number embedded in polymeric structures is to decrease QD mass concentration in the polymer liquid. We investigated this approach with three different concentration of quantum dots (see Supporting Information Section S2).

As already mentioned, the main motivation for this work is to create site-controlled quantum dots as quantum light sources for subsequent use on optical channels. Although the transfer of emission from quantum dots into optical circuits has been shown using various integration methods,^{36–38} DLW-TPP has never been used so far for realizing photonics devices. In order to confirm the potential of our developed approach in this context, we combined ion exchanged waveguides ($1 \times 1 \times 0.3 \text{ cm}^3$) with our QD-polymer nanostructures acting as efficient light sources in the visible wavelength range. Figure 3.(a) shows an SEM image of IEWs. Each waveguide has a width of about 2 μm , a depth of about 2 μm and separated from neighboring waveguides by 51 μm . In our case, surface buried IEWs are beneficial for this application due to their flexibility to be tailored into various applications, with relatively simple and economic fabrication.^{39–41} The 3D schematic of IEW is shown in inset of Figure 3.(a). IEWs have a gradient index profile due to index increment as ion diffuse further into the glass substrate to form waveguides. The refractive index distribution profile and more sample information can be found in Supporting Information Section S3. After the patterning using our developed DLW-TPP platform, QD-polymer nanostructures were fabricated directly at the center of a given waveguide, as shown in Figure 3.(b). The enlarged SEM image in inset shows the details of the QD-polymer nanostructure.

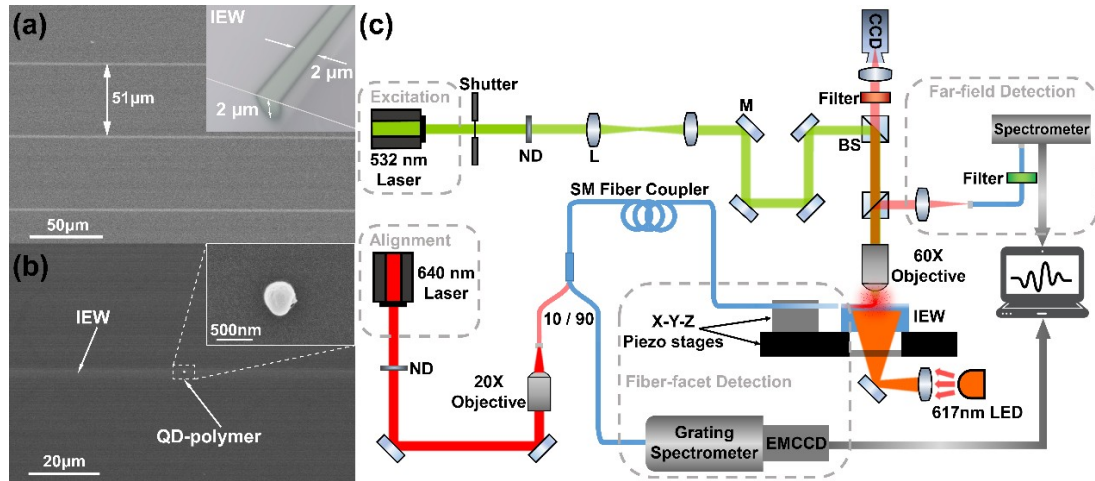


Figure 3. SEM image of IEWs, coated by a conduct carbon layer with 4 nm in thickness. Schematic 3D view of the IEWs shown in inset. (b) Fabricated single QD-polymer voxel at the center of a IEW. Inset shows the enlarged SEM image of this nanostructure. (c) Home-built PL measurement setup consisting of fiber-waveguide coupling stage and spectrum detection systems.

A home-built photoluminescence measurement set-up is used to detect the quantum dot emission coupled to the IEW, as shown in Figure 3.(c). A 617 nm LED light source below the sample stage allows individual devices to be imaged. The input single mode fiber (Thorlabs-630HP, mounted on a x-y-z piezoelectric stage) is aligned at the end of the corresponding waveguide facet with a 640 nm continuous laser to optimize the fiber-IEW coupling. Some of the alignment light is scattered out of the waveguide plane. The spatial distribution of light intensity along the waveguides is projected onto an CCD camera and this allowed us to observe light propagation and to pre-align our waveguides to the optical fiber (as described in Supporting Information Section S4). Once the input fiber is properly aligned, the sample is excited from top simultaneously by switching the excitation laser to 532 nm through a 60× microscope objective (numerical aperture NA = 0.9). The QD emission coupled to the IEWs is collected and detected by a CCD-cooled grating spectrometer. The far-field QD emission can also be collected by a multimode fiber and directed through a 540 nm long-pass filter towards another commercial portable spectrometer (Ocean Optics, QE Pro).

Using our PL measurement set-up, we first measure the far-field quantum dot emission in order to verify that the quantum dots embedded in the polymer nanostructures are still active, as shown in Figure 4.(a). The recorded spectrum shows an apparent peak at 588.5 nm with a FWHM of about 43.1 nm, which is indicative of our CdSe/ZnS QD-like emission signatures. We should also mention that a significant far field QD emission was observed as shown in the inset (red emission spot, filtered by a 580 nm long pass filter). The results show the evidence of the presence of quantum dots inside the polymer nanostructures and their high emission quality.

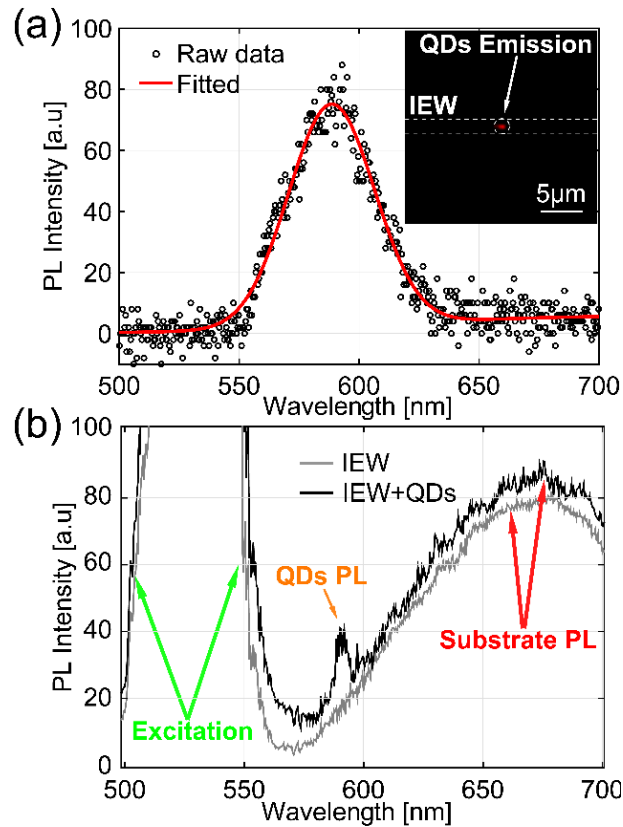


Figure 4. Spectrum of far field quantum dots emission for the single QD-polymer nanostructure on IEW with a Gaussian fit (red line). Inset shows the far field quantum dots emission light (white dashed line represents the outline of the IEW). (b) Normalized extracted spectrum collected from waveguide facet by a single mode fiber. Black line for QD-polymer nanostructure placed on IEW while grey line for IEW without QDs on top.

Finally, we studied the quantum dot emission coupled to the IEW and collected from the waveguide-facet with the optical fiber. [Figure 4.\(b\)](#) shows the extracted spectrum which gives rise to a narrow luminescence peak at 591.1 nm with a FWHM of about 8 nm. The wavelength at maximum intensity is in very good agreement with the far field spectrum presented above. The spectra with high intensity between 500-560 nm represents the 532 nm excitation laser, and the broad spectral emission between 600-700 nm arise by the fluorescence from IEW substrates which is verified by the measured PL spectrum performed on a bare IEW without QD-polymer nanostructure, as plotted in grey solid line. Interestingly, there is a strong discrepancy of PL spectrum FWHM between QD emission into far field and into the IEW. This discordance is related to the dissimilarities in the PL measurement conditions. The IEW guided mode has its energy density maximum underneath the surface. Because of the evanescence of the guided mode above the glass surface,⁴² it is expected that the QD-waveguide coupling efficiency decreases exponentially from the surface to the center of the polymer nanostructure (as simulated in [Supporting Information Section S5](#)). As a consequence, only few to even one single quantum dot localized at very short distances from the waveguide interface might be efficiently coupled to the waveguide. In the other way, far field emission is collected from an ensemble of quantum dots embedded into the polymer voxel. Typically, the emission wavelength is highly related to QD's

diameter.⁴³ This certainly causes an inhomogeneous broadening of the collected emission line shape,^{44–46} resulting in the broad quantum dot emission peak in Figure 4.(a). The size distribution of our quantum dots is analyzed in Supporting Information Section S6. Further investigations will be done to push the limits of the fabrication and characterization process in order to control carefully the number of quantum dots embedded the polymeric nanostructures. For detecting the emission from less quantum dots (even single QDs) coupled to the IEW, it is possible to increase the signal by improving coupling efficiency from quantum dots to IEWs.

To conclude, we demonstrated the capability of our developed DLW-TPP method for enabling on-demand quantum dots positioning on a thick substrate and on a photonic optical chip. Based on this technique, the control of three fabricating parameters, namely, the laser power, the exposure time and the focal height, provides a full control of the QD-polymer voxel size, which is strongly related to the volume of the voxels, all confirmed by far field photoluminescence measurement. Single QD-polymer nanostructures have been successfully integrated at the center of an ion exchanged waveguide. The quantum dot emission was measured from the waveguide facet by our home-build measurement setup. The extracted spectrum of our quantum dot emission showed a narrow peak at 590 nm which is in good agreement with the far field measurement result and suggests that the PL from very few to single quantum dot is efficiently collected by the waveguide. These prove the high potential of QD-polymer nanostructures for nonclassical light sources positioned onto photonic circuits. Future work will focus on improvements of the emission efficiency from quantum dots into the waveguide to enable the efficient detection of quantum dot emission from the waveguide facet for smaller integrated QD-polymer nanostructures. Finally, our developed DLW-TPP technique opens an exciting route for the top-down deterministic integration of quantum dot or other quantum emitters such as colored centers in nanodiamonds within future complex quantum photonic circuits.

■ ASSOCIATED CONTENT

Supporting Information

(1) QD-polymer structures with three different shapes (lines, squares, cubes); (2) The effect of quantum dots mass concentration on far field PL; (3) Refractive index distribution and light propagation mode of ion exchanged waveguide; (4) The details of fiber-waveguide facet alignment; (5) Dependence of quantum dot position on QD-IEW coupling efficiency; (6) QDs size distribution of QD-polymer nanocomposite with single CdSe/ZnS quantum dots layer ([PDF](#))

■ AUTHOR INFORMATION

Corresponding Authors

*E-mail: christophe.couteau@utt.fr

*E-mail: blaize@utt.fr

ORCID

Christophe Couteau: [0000-0001-7676-3205](https://orcid.org/0000-0001-7676-3205)

Safi Jradi: [0000-0003-1712-8986](https://orcid.org/0000-0003-1712-8986)

Renaud Bachelot: [0000-0003-1847-5787](https://orcid.org/0000-0003-1847-5787)

Notes

The authors declare no competing financial interest.

■ ACKNOWLEDGMENTS

This authors acknowledge the support of the ITN (Innovative Training Networks) funded project LIMQUET (Grant agreement ID: 765075) and the Funding of China Scholarship Council (CSC). The authors would like to thank the platform “Nanomat” for nanocharacterization.

■ REFERENCES

- (1) Dietrich, C. P.; Fiore, A.; Thompson, M. G.; Kamp, M.; Höfling, S. GaAs Integrated Quantum Photonics: Towards Compact and Multi-functional Quantum Photonic Integrated Circuits. *Laser Photon. Rev.* **2016**, *10* (6), 870–894.
- (2) Portalupi, S. L.; Hornecker, G.; Giesz, V.; Grange, T.; Lemaître, A.; Demory, J.; Sagnes, I.; Lanzillotti-Kimura, N. D.; Lanco, L.; Auffèves, A. Bright Phonon-Tuned Single-Photon Source. *Nano Lett.* **2015**, *15* (10), 6290–6294.
- (3) Senellart, P.; Solomon, G.; White, A. High-Performance Semiconductor Quantum-Dot Single-Photon Sources. *Nat. Nanotechnol.* **2017**, *12* (11), 1026.
- (4) Claudon, J.; Bleuse, J.; Malik, N. S.; Bazin, M.; Jaffrennou, P.; Gregersen, N.; Sauvan, C.; Lalanne, P.; Gérard, J.-M. A Highly Efficient Single-Photon Source Based on a Quantum Dot in a Photonic Nanowire. *Nat. Photonics* **2010**, *4* (3), 174.
- (5) Sapienza, L.; Davanço, M.; Badolato, A.; Srinivasan, K. Nanoscale Optical Positioning of Single Quantum Dots for Bright and Pure Single-Photon Emission. *Nat. Commun.* **2015**, *6*, 7833.
- (6) Pelton, M.; Santori, C.; Vucković, J.; Zhang, B.; Solomon, G. S.; Plant, J.; Yamamoto, Y. Efficient Source of Single Photons: A Single Quantum Dot in a Micropost Microcavity. *Phys. Rev. Lett.* **2002**, *89* (23), 233602.
- (7) Englund, D.; Fattal, D.; Waks, E.; Solomon, G.; Zhang, B.; Nakaoka, T.; Arakawa, Y.; Yamamoto, Y.; Vučković, J. Controlling the Spontaneous Emission Rate of Single Quantum Dots in a Two-Dimensional Photonic Crystal. *Phys. Rev. Lett.* **2005**, *95* (1), 13904.
- (8) Arcari, M.; Söllner, I.; Javadi, A.; Hansen, S. L.; Mahmoodian, S.; Liu, J.; Thyrrstrup, H.; Lee, E. H.; Song, J. D.; Stobbe, S. Near-Unity Coupling Efficiency of a Quantum Emitter to a Photonic Crystal Waveguide. *Phys. Rev. Lett.* **2014**, *113* (9), 93603.
- (9) Curto, A. G.; Volpe, G.; Taminiau, T. H.; Kreuzer, M. P.; Quidant, R.; van Hulst, N. F. Unidirectional Emission of a Quantum Dot Coupled to a Nanoantenna. *Science* (80-.). **2010**, *329* (5994), 930–933.
- (10) Schnauber, P.; Singh, A.; Schall, J.; Park, S. I.; Song, J. D.; Rodt, S.; Srinivasan, K.; Reitzenstein, S.; Davanco, M. Indistinguishable Photons from Deterministically Integrated Single Quantum Dots in Heterogeneous GaAs/Si₃N₄ Quantum Photonic Circuits. *arXiv Prepr. arXiv1905.12030* **2019**.
- (11) Xie, W.; Gomes, R.; Aubert, T.; Bisschop, S.; Zhu, Y.; Hens, Z.; Brainis, E.; Van Thourhout, D. Nanoscale and Single-Dot Patterning of Colloidal Quantum Dots. *Nano Lett.* **2015**, *15* (11), 7481–7487.
- (12) Woo, C. H.; Beaujuge, P. M.; Holcombe, T. W.; Lee, O. P.; Fréchet, J. M. J. Incorporation of Furan into Low Band-Gap Polymers for Efficient Solar Cells. *J. Am. Chem. Soc.* **2010**, *132* (44), 15547–15549.
- (13) Cui, Y.; Björk, M. T.; Liddle, J. A.; Sönnichsen, C.; Boussert, B.; Alivisatos, A. P. Integration of Colloidal Nanocrystals into Lithographically Patterned Devices. *Nano Lett.* **2004**, *4* (6), 1093–1098.

- (14) Santhosh, K.; Bitton, O.; Chuntunov, L.; Haran, G. Vacuum Rabi Splitting in a Plasmonic Cavity at the Single Quantum Emitter Limit. *Nat. Commun.* **2016**, *7*, ncomms11823.
- (15) Jauffred, L.; Richardson, A. C.; Oddershede, L. B. Three-Dimensional Optical Control of Individual Quantum Dots. *Nano Lett.* **2008**, *8* (10), 3376–3380.
- (16) Jensen, R. A.; Huang, I.-C.; Chen, O.; Choy, J. T.; Bischof, T. S.; Lončar, M.; Bawendi, M. G. Optical Trapping and Two-Photon Excitation of Colloidal Quantum Dots Using Bowtie Apertures. *ACS Photonics* **2016**, *3* (3), 423–427.
- (17) Zadeh, I. E.; Elshaari, A. W.; Jöns, K. D.; Fognini, A.; Dalacu, D.; Poole, P. J.; Reimer, M. E.; Zwiller, V. Deterministic Integration of Single Photon Sources in Silicon Based Photonic Circuits. *Nano Lett.* **2016**, *16* (4), 2289–2294.
- (18) Kim, J.-H.; Aghaeimeibodi, S.; Richardson, C. J. K.; Leavitt, R. P.; Englund, D.; Waks, E. Hybrid Integration of Solid-State Quantum Emitters on a Silicon Photonic Chip. *Nano Lett.* **2017**, *17* (12), 7394–7400.
- (19) Kress, S. J. P.; Richner, P.; Jayanti, S. V.; Galliker, P.; Kim, D. K.; Poulikakos, D.; Norris, D. J. Near-Field Light Design with Colloidal Quantum Dots for Photonics and Plasmonics. *Nano Lett.* **2014**, *14* (10), 5827–5833.
- (20) Siampour, H.; Kumar, S.; Bozhevolnyi, S. I. Nanofabrication of Plasmonic Circuits Containing Single Photon Sources. *Acs Photonics* **2017**, *4* (8), 1879–1884.
- (21) Sun, H.-B.; Takada, K.; Kim, M.-S.; Lee, K.-S.; Kawata, S. Scaling Laws of Voxels in Two-Photon Photopolymerization Nanofabrication. *Appl. Phys. Lett.* **2003**, *83* (6), 1104–1106.
- (22) Von Freymann, G.; Ledermann, A.; Thiel, M.; Staude, I.; Essig, S.; Busch, K.; Wegener, M. Three-dimensional Nanostructures for Photonics. *Adv. Funct. Mater.* **2010**, *20* (7), 1038–1052.
- (23) Cumpston, B. H.; Ananthavel, S. P.; Barlow, S.; Dyer, D. L.; Ehrlich, J. E.; Erskine, L. L.; Heikal, A. A.; Kuebler, S. M.; Lee, I.-Y. S.; McCord-Maughon, D. Two-Photon Polymerization Initiators for Three-Dimensional Optical Data Storage and Microfabrication. *Nature* **1999**, *398* (6722), 51.
- (24) Farsari, M.; Chichkov, B. N. Materials Processing: Two-Photon Fabrication. *Nat. Photonics* **2009**, *3* (8), 450.
- (25) Maruo, S.; Nakamura, O.; Kawata, S. Three-Dimensional Microfabrication with Two-Photon-Absorbed Photopolymerization. *Opt. Lett.* **1997**, *22* (2), 132–134.
- (26) Smith, M. J.; Lin, C. H.; Yu, S.; Tsukruk, V. V. Composite Structures with Emissive Quantum Dots for Light Enhancement. *Adv. Opt. Mater.* **2019**, *7* (4), 1801072.
- (27) Park, J.-J.; Prabhakaran, P.; Jang, K. K.; Lee, Y.; Lee, J.; Lee, K.; Hur, J.; Kim, J.-M.; Cho, N.; Son, Y. Photopatternable Quantum Dots Forming Quasi-Ordered Arrays. *Nano Lett.* **2010**, *10* (7), 2310–2317.
- (28) Krini, R.; Ha, C. W.; Prabhakaran, P.; Mard, H. El; Yang, D.; Zentel, R.; Lee, K. Photosensitive Functionalized Surface-Modified Quantum Dots for Polymeric Structures via Two-Photon-Initiated Polymerization Technique. *Macromol. Rapid Commun.* **2015**, *36* (11), 1108–1114.
- (29) Park, S.-K.; Teng, X.; Jung, J.; Prabhakaran, P.; Ha, C. W.; Lee, K.-S. Photopatternable Cadmium-Free Quantum Dots with Ene-Functionalization. *Opt. Mater. Express* **2017**, *7* (7), 2440–2449.
- (30) Peng, Y.; Jradi, S.; Yang, X.; Dupont, M.; Hamie, F.; Dinh, X. Q.; Sun, X. W.; Xu, T.;

- Bachelot, R. 3D Photoluminescent Nanostructures Containing Quantum Dots Fabricated by Two-Photon Polymerization: Influence of Quantum Dots on the Spatial Resolution of Laser Writing. *Adv. Mater. Technol.* **2019**, *4* (2), 1800522.
- (31) Obata, K.; El-Tamer, A.; Koch, L.; Hinze, U.; Chichkov, B. N. High-Aspect 3D Two-Photon Polymerization Structuring with Widened Objective Working Range (WOW-2PP). *Light Sci. Appl.* **2013**, *2* (12), e116.
- (32) Bückmann, T.; Stenger, N.; Kadic, M.; Kaschke, J.; Frölich, A.; Kennerknecht, T.; Eberl, C.; Thiel, M.; Wegener, M. Tailored 3D Mechanical Metamaterials Made by Dip-In Direct Laser-Writing Optical Lithography. *Adv. Mater.* **2012**, *24* (20), 2710–2714.
- (33) Zhou, X.; Hou, Y.; Lin, J. A Review on the Processing Accuracy of Two-Photon Polymerization. *AIP Adv.* **2015**, *5* (3), 30701.
- (34) Sun, H.-B.; Maeda, M.; Takada, K.; Chon, J. W. M.; Gu, M.; Kawata, S. Experimental Investigation of Single Voxels for Laser Nanofabrication via Two-Photon Photopolymerization. *Appl. Phys. Lett.* **2003**, *83* (5), 819–821.
- (35) Sun, H.-B.; Kawata, S. Two-Photon Photopolymerization and 3D Lithographic Microfabrication. In *NMR•3D Analysis•Photopolymerization*; Springer, 2004; pp 169–273.
- (36) Davanco, M.; Liu, J.; Sapienza, L.; Zhang, C.-Z.; Cardoso, J. V. D. M.; Verma, V.; Mirin, R.; Nam, S. W.; Liu, L.; Srinivasan, K. Heterogeneous Integration for On-Chip Quantum Photonic Circuits with Single Quantum Dot Devices. *Nat. Commun.* **2017**, *8* (1), 889.
- (37) Chen, B.; Wu, H.; Xin, C.; Dai, D.; Tong, L. Flexible Integration of Free-Standing Nanowires into Silicon Photonics. *Nat. Commun.* **2017**, *8* (1), 20.
- (38) Rao, V. S. C. M.; Hughes, S. Single Quantum Dot Spontaneous Emission in a Finite-Size Photonic Crystal Waveguide: Proposal for an Efficient “on Chip” Single Photon Gun. *Phys. Rev. Lett.* **2007**, *99* (19), 193901.
- (39) Tervonen, A.; Honkanen, S. K.; West, B. R. Ion-Exchanged Glass Waveguide Technology: A Review. *Opt. Eng.* **2011**, *50* (7), 71107.
- (40) Jordan, E.; Geoffray, F.; Bouchard, A.; Ghibaudo, E.; Broquin, J.-E. Development of Tl⁺/Na⁺ Ion-Exchanged Single-Mode Waveguides on Silicate Glass for Visible-Blue Wavelengths Applications. *Ceram. Int.* **2015**, *41* (6), 7996–8001.
- (41) Varsanik, J. S.; Bernstein, J. J. Integrated Optic/Nanofluidic Fluorescent Detection Device with Plasmonic Excitation. *J. Micromechanics Microengineering* **2013**, *23* (9), 95017.
- (42) Snyder, A. W.; Love, J. *Optical Waveguide Theory*; Springer Science & Business Media, 2012.
- (43) Alivisatos, A. P. Semiconductor Clusters, Nanocrystals, and Quantum Dots. *Science* (80-.). **1996**, *271* (5251), 933–937.
- (44) Cui, J.; Beyler, A. P.; Coropceanu, I.; Cleary, L.; Avila, T. R.; Chen, Y.; Cordero, J. M.; Heathcote, S. L.; Harris, D. K.; Chen, O. Evolution of the Single-Nanocrystal Photoluminescence Linewidth with Size and Shell: Implications for Exciton–Phonon Coupling and the Optimization of Spectral Linewidths. *Nano Lett.* **2015**, *16* (1), 289–296.
- (45) van der Stam, W.; de Graaf, M.; Gudjonsdottir, S.; Geuchies, J. J.; Dijkema, J. J.; Kirkwood, N.; Evers, W. H.; Longo, A.; Houtepen, A. J. Tuning and Probing the Distribution of Cu⁺ and Cu²⁺ Trap States Responsible for Broad-Band Photoluminescence in CuInS₂ Nanocrystals. *ACS Nano* **2018**, *12* (11), 11244–11253.
- (46) Whitham, P. J.; Marchioro, A.; Knowles, K. E.; Kilburn, T. B.; Reid, P. J.; Gamelin, D. R. Single-Particle Photoluminescence Spectra, Blinking, and Delayed Luminescence of Colloidal

CuInS₂ Nanocrystals. *J. Phys. Chem. C* **2016**, *120* (30), 17136–17142.